

Experimental Study of a Liquid Fuel-fired Porous Radiant Burner (LPRB)

Sumreng Jugjai^{*}, Makorn Lakkana, Yossapong Laonual

Combustion and Engine Research Laboratory (CERL),
Mechanical Engineering Department, Faculty of Engineering, King Mongkut's University of Technology Thonburi
(KMUTT), Bangkok, 10140, Thailand,

Tel: 0-66470-9128, Fax: 0-66470-9111, ^{*}E-mail: sumrueng.jug@kmutt.ac.th

Abstract

This paper presents the results of an experimental investigation performed upon a novel liquid fuels-fired porous radiant burner (LPRB) fuelled by liquid kerosene without atomization. The main goal of this research activity was a systematic investigation of the burner aimed at finding the best operating conditions with low pollutant emissions. The analysis has been carried out for different inter-distance between the up- and downstream porous media. To significantly reduce pollutant emissions as the same time with increasing a radiant output, the LPRB has to be operated based on a fully matrix-stabilized flame (MSF) within the porous medium. This MSF has been favored through an annular combustion air supply into the downstream porous medium obtained by an adjustable upstream porous medium and a subsequent removal of the inter-distance between them. The most important result of this solution was a substantial NO_x reduction of the order of 50% with respect to the original burner configuration, which could be achieved by means of the MSF. LPRB offers a high potential to replace conventional spray combustion systems.

Keywords: Porous radiant burner (PRB), Porous inert medium (PIM), Liquid fuels combustion, NO_x reduction

1. Introduction

A novel liquid fuels-fired porous radiant burner (hereafter referred to as LPRB) without atomization is presented. In the past, LPRB was focused on combustion took place outside the burner to its downstream end with an open flame, whereas evaporation completely took place within the porous burner [1].

This is undesirable for practical application of the porous burner. A method allowing simultaneous evaporation and combustion to take place within the burner is of special importance for its high combustion efficiency and high radiation output.

In order to solve the problems with state-of-the-art technology, a new LPRB that could be operated with the phenomenon of evaporation and combustion simultaneously taking place within the inert porous medium burner and without the need of a fine droplet atomization has been proposed [2]. The burner can be considered as down-flow and non-premixed. It consisted of two cylindrical porous media with different pore size. They were stacked together but with a small space in-between for a mixing chamber. The concept is based on an evaporation of liquid fuel in an upstream porous medium (hereafter referred to as a porous burner PB), a subsequent mixing with the combustion air in the mixing chamber and the final combustion in a downstream porous medium (hereafter referred to as a porous emitter PE). During normal operation, the evaporation is maintained through the upstream heat transfer by intense thermal radiation emitted from the PE to the PB. With this arrangement, evaporation within PB is thus completely separated from combustion, resulting in a nearly homogeneous mixture of fuel vapor and air to be formed in the mixing chamber followed by a nearly homogeneous combustion within PE afterwards.

In our previous experimental study [2], however, the size of the mixing chamber, which is specified by the PB to PE inter-distance X_{PB} (Fig. 2), was fixed and was not small enough to clarify the effect on thermal structure and combustion characteristics. To clarify the effect of size of the mixing chamber, and to broaden the base for future research, this

experimental study was carried out.

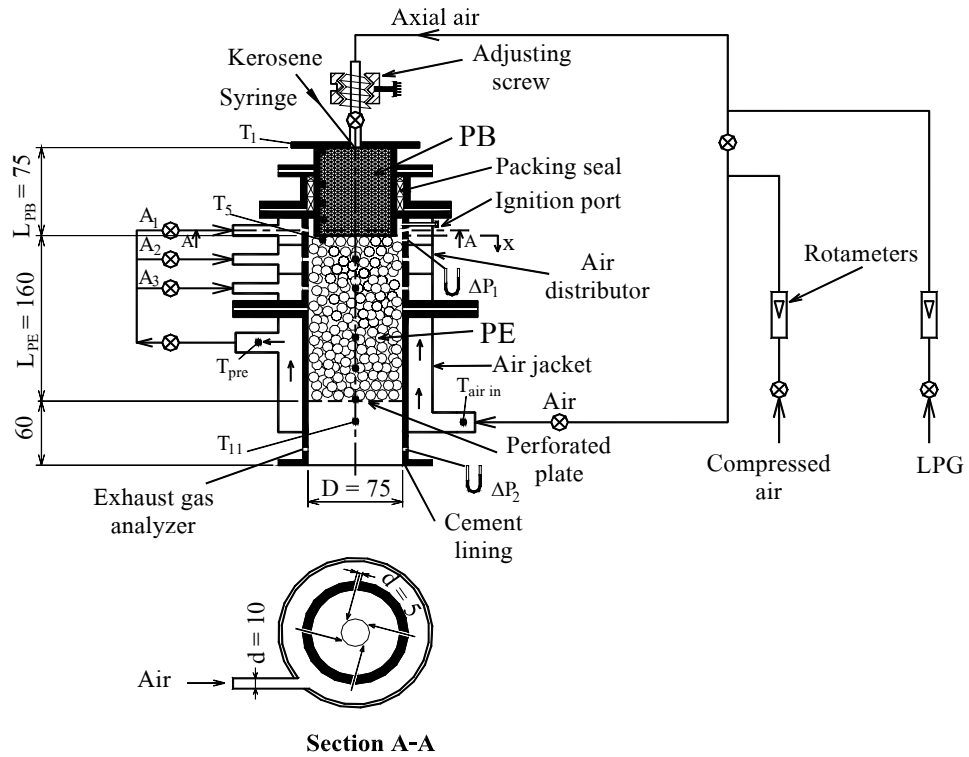


Fig. 1. Experimental setup of LFPB.

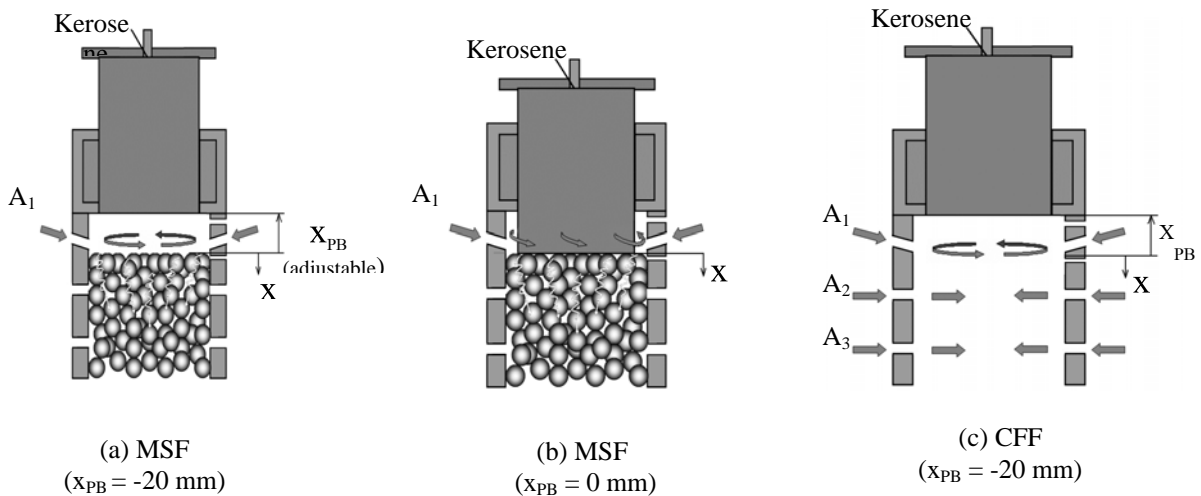


Fig. 2. Details of air supply of LFPB.

2. Experiments

2.1 Apparatus

Fig. 1 shows an experimental setup of the proposed LFPB, and Fig. 2 shows details of its air supply. The LFPB is arranged

in a down-flow combustor, consisting of two main components, i.e. a porous burner (PB) for evaporation and a porous emitter (PE) for combustion. This design is an improvement over the previous one [2]. A special characteristic of the construction of

the new LFPB is that it allows a change of axial position of PB with respect to the position of PE, which is fixed at a specific location. The position of PB can be independently adjusted by turning an adjusting screw mounted at the upstream end of PB as shown in Fig. 1. By taking the upstream surface of PE as a reference position, i.e. $x = 0$, the position of PB with respect to PE is defined by the PB to PE inter-distance X_{PB} as shown in Fig. 2(a). X_{PB} is designed in such a way that it could be adjusted from -20 mm to 0 mm without the problem of supplying the combustion air as occurred in the original design [2]. With $X_{PB} = -20$ mm, a mixing chamber is formed in between the PB and PE as shown in Fig. 2(a), whereas the mixing chamber is completely removed with $X_{PB} = 0$ mm as shown in Fig. 2(b). With this design accompanied by a smaller diameter of PB than PE, an annular chamber was formed around the circumference of the PB, allowing the swirling air (A_1) to be supplied and diffused through the PE before mixing with the fuel vapor. Therefore, blockage of the swirling air exit that may be caused by the leading edge of the PB as is occurred in the original design could be avoided, ensuring a fully matrix-stabilized flame to be occurred within the PE. This can be considered as one step further from the original burner design [2].

The LFPB is arranged in such a way that either a matrix-stabilized flame (MSF) within the PE or a conventional combustion system with free flame (CFF) could be established depending on the arrangement. With PE installed downstream of PB as shown by Figs 2(a) or 2(b), the combustion is characterized as the MSF, otherwise it is considered as the CFF as shown by Fig. 2(c). Both PB and PE are encased by cylindrical steel tubes having internal surfaces lined with high-temperature cement. The external surface of the PE section is covered by an air jacket for preheating the combustion air. The preheated combustion air is then divided into three airflows, i.e. A_1 , A_2 and A_3 , before being fed to each corresponding air distributor surrounding the combustion zone as shown in Fig. 1. Then, each airflow is injected into the combustion zone through injector ports drilled into the side wall within the air distributors.

Different combustion regimes require different airflows. With the MSF mode, however, A_2 and A_3 are not employed, for the sake of favorable combustion characteristics. The total preheated combustion air is supplied as A_1 , as shown in Figs 2(a) and 2(b) irrespective of X_{PB} . On the other hand, with the CFF mode, the total preheated combustion air is divided into A_1 , A_2 and A_3 (Fig. 2(c)) with equal flow rate obtained by pre-adjusting the metering valves. Each airflow has its own flow pattern. A_1 is supplied

tangentially into the mixing chamber through four small ports having diameter $d = 5$ mm, resulting in a four-way swirling air directed towards the circumference of a small, imaginary circle at the center of the mixing chamber for obtaining good mixing along the circumference direction (section A-A in Fig. 1). On the other hand, A_2 and A_3 are supplied in the radial direction and directed to the center of the mixing chamber through four small ports, forming a four-way impinging air jet, ensuring good mixing in the central core region (Fig. 2(c)).

Even though the PB does not contain a combustion zone as its name implies, it is the PB that causes evaporation followed by combustion near its exit. Therefore, we retain the name "porous burner PB" so as to reflect its main contribution to combustion via its true function as an evaporator. Fundamentally, the PB is a phase-change problem in its solid matrix of which its downstream surface is subjected to an intense thermal radiation emitted from flame or from PE for evaporation within PB, whereas its upstream one is supplied with liquid kerosene through a syringe without atomization. Kerosene in the storage tank is pressurized by nitrogen gas at relatively low pressure (about 1 atm), which is just enough to cause the kerosene to flow to the syringe. The PB consists of a packed bed of circular pieces of metallic wire screen. Based on our preliminary experiment, it was found that the metallic wire screen of 100 mesh/inch is sufficient to produce efficient evaporation with uniform distribution of the fuel vapor at the PB exit. This is equivalent to an optical thickness (τ_{PB}) of about 131. τ_{PB} is a dimensionless parameter noting the amount of thermal radiation energy absorbed or emitted by the PB, and is equal to the multiplication between an extinction coefficient (which is taken here as an absorption coefficient K_{PB}) and the geometric length of the PB ($L_{PB} = 75$ mm). Detailed specific data of the PB and its wire screen is given in Tab. 1.

In contrast to the PB, the PE consists of a packed bed of randomly arranged spherical inert alumina particles with average diameter of about 10 mm. The length of PE is $L_{PE} = 160$ mm with its downstream end supported by a perforated plate made of a heat-resisting steel. The purpose of the PE is to provide an energy feedback mechanism by thermal radiation to the PB for continuous evaporation and serve as a radiant burner wherein combustion takes place with thermal radiation energy directed towards its downstream exit for practical utilizations. Detailed specific data of the particles for PE is also given in Tab. 1.

2.2 Measurement

The combustion characteristics are determined from profiles of the temperature along the burner length and the composition

of the combustion gases at the burner exit. The thermocouple readings are just for the thermocouples alone. However, they can be used to estimate the porous medium (or solid) temperatures, not the flame gas temperatures, since the thermocouples are also solid by themselves. Temperature measurements (T_1 - T_{11}) within the porous media of PB and PE were made using an array of two different types of thermocouples with their junctions (represented by solid circles) positioned at any radial position depending on section (Fig. 1). In the PE section, wherein a very high temperature (up to $1,600^\circ\text{C}$) exists because of combustion, six bare thermocouples (T_6 - T_{11}) of Pt/Pt-13%Rh having 0.25-mm diameter were used (Fig. 1). They were inserted through small ports in the burner wall with their junctions positioned at the centerline of the burner. In contrast to the PE, the PB section, wherein relatively low temperatures exist because of evaporation, was instrumented by an array of five N-type sheathed thermocouples (T_1 - T_5) with 1.5-mm diameter (Fig. 1). These sheathed thermocouples were inserted through a small gap at the interface between the cement lining and the PB with their junctions positioned at different locations along the interface. This is to prevent the liquid fuel flow pattern within the PB from being disturbed by protrusion of the thermocouple junctions. There are also two N-type sheathed thermocouples of $T_{\text{air in}}$ and T_{pre} , which are located, respectively, at inlet and outlet of the air jacket for measuring the inlet temperature and the preheat temperature of the combustion air. Signals of all the thermocouples are digitized by a general-purpose data logger and then transmitted to a personal computer. Upon reaching steady-state condition for each experimental condition, thermocouple readings for each location were almost flat with relatively small perturbation. Then the temperatures were averaged over a specific time interval and plotted on a graph.

Emission analysis at the LFPB exit is carried out by using the Messtechnik Eheim model Visit01L, which is a portable emission analyzer designed specifically for quasi-continuous measurement. A gas processing system of total NO_x and CO is specifically tuned for electrochemical sensors, ensuring long-time stability and accuracy of measurement. The measuring range of the analyzer is 0-4,000 ppm for NO_x and 0-10,000 ppm for CO with measuring accuracy of about ± 5 ppm (from the measured value) and resolution of 1 ppm for both NO_x and CO. All measured emissions in the experiment are those corrected to dry, air-free values. Calibrated rotameters were used to measure flow rate of the liquid kerosene and flow rate of the combustion air. Pressure difference ΔP_1 and ΔP_2 were measured by standard manometers. Repeated measurement shows an uncertainty of

about 10% for both the species concentrations and the temperature.

Tab. 1. Operating conditions.

Absorption coefficient of PB, K_{PB}	=1,750 1/m
Absorption coefficient of PE, K_{PE}	=19.8 1/m
Average sphere diameter of PE, d_{PE}	=10 mm
Length of PB, L_{PB}	= 75 mm
Length of PE, L_{PE}	= 160 mm
Lower heating value of kerosene, LHV	= 43,124 kJ/kg
Mesh/inch of wire screen for PB	100 mesh/inch
Optical thickness of PB, $\tau_{\text{PB}} = K_{\text{PB}}L_{\text{PB}}$	= 131
Optical thickness of PE, $\tau_{\text{PE}} = K_{\text{PE}}L_{\text{PE}}$	= 4.2
Pitch of metallic wire screen for PB, p_{PB}	= 0.254 mm
Porosity of PB, ε	=0.61
Specific interfacial area of PB, a	=12,368 m^2/m^3
Wire diameter of wire screen for PB, d_w	= 0.125 mm

2.3 Procedure

A non-premixed mixture of LPG and air is supplied through the PE for preheating with the entire combustion air comes from the air flowing through the air jacket, whereas the LPG is supplied through the PB. Ignition is initiated by inserting a pilot oxy-acetylene flame through an ignition port. By adjusting flow rate of the combustion air with an appropriate overall equivalence ratio Φ , a luminous, turbulent, diffusion flame stabilized near the exit of the PB (CFF) or a matrix-stabilized, non-premixed flame (MSF) within the PE can be achieved. Then, the combustion air is increased to an amount corresponding to the kerosene flow rate (or firing rate CL) to be subsequently supplied by admixing with the LPG in the PB. With a suitable value of Φ , a kerosene flame can be achieved, and the LPG is then gradually decreased until it is completely turned off. During this course, the overall equivalence ratio Φ is readjusted by adjusting the combustion air in such a way that stable combustion of the kerosene flame is maintained while promoting complete combustion. As a steady-state condition was reached, T , ΔP and concentrations of CO and NO_x at the LFPB exit were recorded.

3. Results and discussion

Fig. 3 shows typical temperature profiles of MSF at different X_{PB} . A typical temperature profile of CFF at an identical experimental condition was also included for comparison. With PE installed at an initial $X_{\text{PB}} = -20$ mm, it is clear that the combustion regime has been changed from a combustion with

free flame (CFF) to a matrix-stabilized one (MSF) because the position of the combustion zone, where the maximum temperature T_{max} is located, is displaced into the PE at $x = 20$ mm. It is interesting to note that the excess enthalpy combustion regime [3] of MSF becomes more pronounced with T_{max} far exceeding the corresponding T_{ad} and T_{max} of the CFF. This is attributed to an efficient heat re-circulation from products to reactant (liquid fuel and air) by thermal radiation emitted from PE to PB. Thus, enhanced evaporation followed by a fast burning velocity could be expected for the MSF mode. However, the combustion pressure is fairly high with $\Delta P_1 = 280$ mmH₂O as compared with that of the CFF, which is almost equal to the ambient pressure. Reduction in the inter-distance to $X_{PB} = -10$ mm increases the temperature throughout the combustor length with the combustion zone fixed at the same position ($x = 20$ mm).

Further reduction in X_{PB} to a minimum possible value of $X_{PB} = 0$ mm results in a shift in the combustion zone deeper inside the PE to $x = 45$ mm simultaneously with a significant decrease in T_{max} but a marked increase in temperature at the downstream region of the PE (Fig. 3). Moreover, this is accompanied by higher T_5 and T_{pre} as shown in Fig. 4. Pressure difference ΔP_1 slightly decreases with X_{PB} . At $X_{PB} = 0$ mm comes the first experimental results of liquid fuel combustion through inert porous media, wherein evaporation, mixing and combustion are simultaneously taking place within them without the need of atomization. Evaporation is fully completed within the porous burner PB, whilst the flame is fully stabilized within the porous emitter PE, with thermal structure in terms of temperature profile behaving very much like that of the premixed flame stabilized within a bi-layer porous medium.

As the flame location shifts deeper inside the PE by decreasing the X_{PB} , the MSF has shown a simultaneous decrease in CO and total NO_x as shown in Fig. 5. The deeper the combustion zone of MSF moves into the PE, the more complete combustion would become with reduction of total NO_x emission. Lowering in CO emissions may be attributed to lowering in the maximum flame temperature as the flame moved deeper into the PE simultaneously with an increase in radiation losses downstream of PE. This is true for CO formation. CO is reduced if the radiation is extracted from PE to the surrounding area, leading to the lower maximum temperature. Conversely, CO increases if such radiated energy is retained within the porous burner interior and is trapped, resulting in an increased maximum

flame temperature. At $X_{PB} = 0$ mm, the MSF yields almost the same CO emission as that of the CFF.

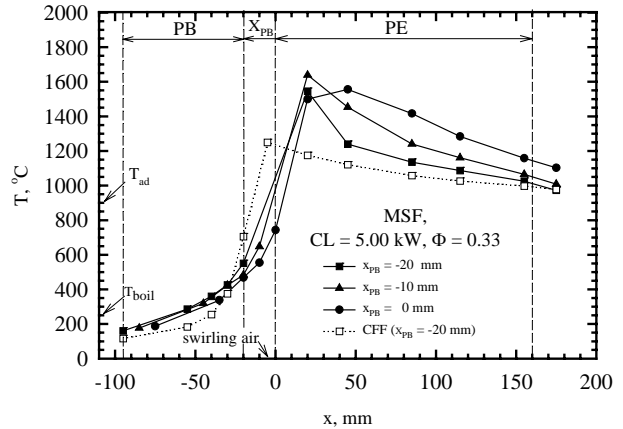


Fig. 3. Effect of X_{PB} on flame structure of MSF.

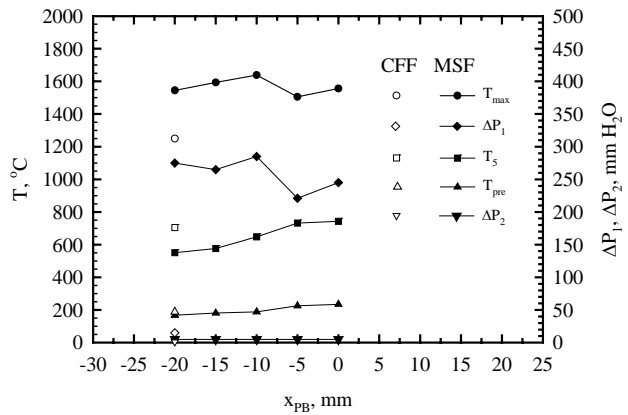


Fig. 4. Effect of X_{PB} on T_{max} , T_5 , T_{pre} and ΔP .

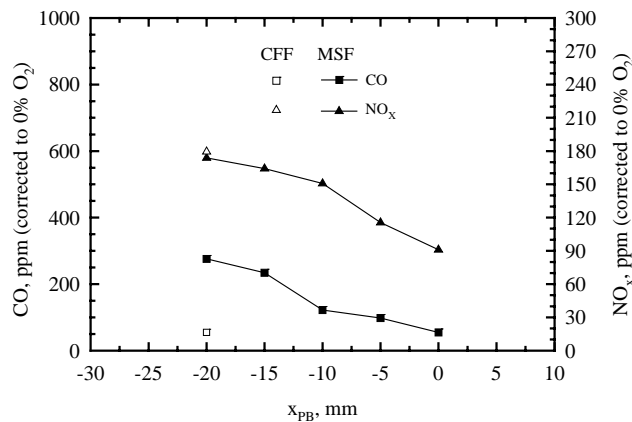


Fig. 5. Effect of X_{PB} on CO and NO_x.

Regarding total NO_x emissions, both the thermal and prompt mechanisms contributed to NO_x formation in porous media burner [4]. At $X_{PB} = 0$ mm, the MSF yields total NO_x emissions of the order of 50% of the CFF at the same experimental conditions. This can be explained by two reasons. Firstly, the quenching effect caused by radiation losses in the combustion zone within the porous matrix of PE plays a significant role in decreasing the maximum combustion temperature (Figs. 3 and 4). Both solid and gas radiation losses directed towards up- and downstream direction of PE in the combustion zone and in the post-combustion zone within the porous matrix of PE, where the concentrations of CO₂ and H₂O are produced, play an important role in quenching the combustion gases. Thus, thermal NO_x and prompt NO_x could be reduced significantly when the combustion temperature is reduced, for the same reasons as those for the reduction in CO as described above.

Secondly, total NO_x reduction may be attributed to a remarkable decrease in prompt NO_x cause by an effect of a continuous staged combustion in a porous inert medium of PE [5]. With the special feature of this LFPB, a continuous staged combustion can be established within the PE because the combustion air is continuously fed through an annular chamber (Fig. 2(b)). The air flows laterally along the circumference of the porous medium of PE. Either lean/lean or rich/lean combustion can take place within the PE. Even a combination of the two may also be possible because of complex fluid mechanics in terms of flow velocities and turbulence in porous media. With a radial velocity component created within a porous medium [6], a layer of cross mixing between the air flowing at the outer annular and the fuel vapor flowing in the inner core of PE can be formed,

resulting in a continuous staged combustion throughout the circumference of PE. The reaction products leaving an initial stage near the PB exit are subsequently mixed with fuel vapor and air in the following stage along the lateral direction of the PE until the combustion is completed.

NO_x produced in this combustion with MSF was mainly prompt NO_x [5]. It was found that this NO_x concentration is insensitive to the combustion temperature. Even when the combustion temperature of the continuous staged combustion within a porous medium burner was lowered considerably by increasing the combustion air (or air-feeding combustion), NO_x

remained constant. This proves that thermal NO_x mechanisms are of minor influence and the major part of the total NO_x is formed within the PE by prompt-NO_x mechanisms.

4. Conclusion

Operating the LFPB with fully stabilized flame of MSF mode yields a more pronounced heat re-circulating combustion characteristic as compared with conventional combustion with free flame CFF mode. With the PB to PE inter-distance becoming progressively smaller, the CO and the NO_x level simultaneously decrease with the shift in location of combustion zone deep inside the PE. Substantial NO_x reduction of the order of 50% with respect to the CFF mode could be achieved by means of a fully matrix-stabilized flame implemented by the proposed unique annular combustion air supply through the PE. The proposed LFPB can be considered as a low NO_x burner for liquid fuels combustion capable of replacing the rival spray combustion.

References

- [1] Takami, H., Suzuki, T., Itaya, Y., and Hasatani, M., 1998. Performance of flammability of kerosene and NO_x emission in the porous burner. *Fuel*, Vol. 77, No. 3, pp. 165-171.
- [2] Jugjai, S., and Polmart, N., 2003. Enhancement of evaporation and combustion of liquid fuels through porous media. *Exp. Therm. Fluid Sci.*, Vol. 27, No. 8, pp. 901-909.
- [3] Weinberg, F.J., 1971. Combustion temperatures: the future? *Nature*, Vol. 233, pp. 239-241.
- [4] Bouma, P.H., Eggels, R.L., De Goey, L.P.H., Nieuwenhuizen, J.K., and Drift, A.V., 1995. A numerical and experimental

study of NO-emission of ceramic foam surface burners.
Combust. Sci. Technol., Vol. 108, pp. 193-203.

- [5] Pickenäcker, O., Kesting, A. and Trimis, D., 2000. Novel low NO_x burner designs for boilers and furnaces by using staged combustion in inert porous media. 5th European Conference on Industrial Furnace and Boilers INFUB5, Espinho-Porto, Portugal, Vol. 1, pp. 1-12.
- [6] Kufner, R., and Hofmann, H., 1990. Implementation of radial porosity and velocity distribution in a reactor model for heterogeneous catalytic gas phase reactions. Chem. Engr. Sci., Vol. 45, No. 8, pp. 2141-2146.